Membrane damage by human islet amyloid polypeptide through fibril growth at the membrane

Maarten F. M. Engel*†‡, Lucie Khemtémourian†, Cécile C. Kleijer†, Hans J. D. Meeldijk§, Jet Jacobs*¶, Arie J. Verkleij§, Ben de Kruijff†, J. Antoinette Killian†, and Jo W. M. Höppener*

*Department of Metabolic and Endocrine Diseases, Division of Biomedical Genetics, and ¶Division of Laboratories and Pharmacy, University Medical Center Utrecht, P. O. Box 85090, 3508 AB Utrecht, The Netherlands; †Research Group Biochemistry of Membranes, Bijvoet Institute, Institute of Biomembranes, and §Department of Cellular Architecture and Dynamics, Utrecht University, Padualaan 8, 3584 CH Utrecht, The Netherlands

Fibrillar protein deposits (amyloid) in the pancreatic islets of Langerhans are thought to be involved in death of the insulin-producing islet β cells in type 2 diabetes mellitus. It has been suggested that the mechanism of this β cell death involves membrane disruption by human islet amyloid polypeptide (hIAPP), the major constituent of islet amyloid. However, the molecular mechanism of hIAPP-induced membrane disruption is not known. Here, we propose a hypothesis that growth of hIAPP fibrils at the membrane causes membrane damage. We studied the kinetics of hIAPP-induced membrane damage in relation to hIAPP fibril growth and found that the kinetic profile of hIAPP-induced membrane damage is characterized by a lag phase and a sigmoidal transition, which matches the kinetic profile of hIAPP fibril growth. The observation that seeding accelerates membrane damage supports the hypothesis. In addition, variables that are well known to affect hIAPP fibril formation, i.e., the presence of a fibril formation inhibitor, hIAPP concentration, and lipid composition, were found to have the same effect on hIAPP-induced membrane damage. Furthermore, electron microscopy analysis showed that hIAPP fibrils line the surface of distorted phospholipid vesicles, in agreement with the notion that hIAPP fibril growth at the membrane and membrane damage are physically connected. Together, these observations point toward a mechanism in which growth of hIAPP fibrils, rather than a particular hIAPP species, is responsible for the observed membrane damage. This hypothesis provides an additional mechanism next to the previously proposed role of oligomers as the main cytotoxic species of amyloidogenic proteins.

amylin | amyloid cytotoxicity | large unilamellar vesicles | protein–membrane interaction | type 2 diabetes mellitus

Type 2 diabetes mellitus (DM2) is characterized histopathologically by the presence of fibrillar amyloid deposits in the pancreatic islets of Langerhans. Amyloid cytotoxicity is thought to be an early mechanism involved in death of insulin-producing islet β cells in DM2 (1). The main component of islet amyloid, and the actual fibril-forming molecule, is a 37-amino acid peptide called human islet amyloid polypeptide (hIAPP) or amylin, which is produced together with insulin in the pancreatic islet β-cells. It is thought that β cells of DM2 patients are somehow killed through hIAPP-induced damage of the β cell membrane (2). However, our knowledge of the mechanism of hIAPP-induced membrane damage is extremely sparse. It is not known how cytotoxic hIAPP species interact with cellular membranes and induce cell death. Furthermore, it is not established whether cytotoxic hIAPP species are formed before contacting the membrane or whether a membrane environment is in fact required for the formation of cytotoxic hIAPP species.

The prevailing view is that membrane damage and concomitant β cell death are caused by cytotoxic hIAPP oligomers (2–9). There are indications that these oligomers form ion channels (2, 3), as has been suggested for other amyloidogenic proteins (10, 11). Other studies indicate that hIAPP-induced membrane damage is not specific for ions, but results in membrane leakage of molecules the size of calcein (600 Da), indicating a general membrane disruption mechanism (9, 12–15). In addition to the hypothesis that oligomers are the toxic species, recent reports suggest that the fibrillar form of amyloidogenic proteins can also be cytotoxic, e.g., fibrillar Abeta1–40 (16), fibrillar prion protein (17), and fibrillar lysozyme (18). Thus, not only is the mechanism of cytotoxic action of amyloidogenic proteins unknown, the nature of the cytotoxic species is still a topic of discussion as well.

Previously, we observed by confocal light microscopy that hIAPP-induced loss of membrane barrier function is accompanied by the appearance of Congo red-positive protein aggregates at the phospholipid bilayer of giant unilamellar vesicles (12). This finding suggests that membrane damage may be related to the process of hIAPP fibril growth. Here, we explored this possibility further by investigating the kinetics of hIAPP-induced membrane disruption in relation to hIAPP fibril growth. Although membrane disruption by hIAPP has been quantified before (4, 9, 14), up until now the kinetics of this process and its relation to fibril growth have received only marginal attention. Our results lead to the hypothesis that hIAPP fibril growth at the membrane can cause hIAPP-induced membrane disruption. This hypothesis provides a mechanism complementary to the existing notion that hIAPP oligomers are the cytotoxic species responsible for membrane damage.

Results

Matching Kinetic Profiles of hIAPP-Induced Membrane Leakage and hIAPP Fibril Formation. To gain insight into the possible relationship between hIAPP-induced membrane damage and hIAPP fibril formation, we measured the kinetics of hIAPP-induced membrane damage and compared it with the kinetics of hIAPP fibril growth under various experimental conditions. Membrane damage was quantitatively and *in situ* determined by allowing hIAPP fibril formation in the presence of calcein-filled large unilamellar vesicles (LUVs), an established membrane leakage assay, which has been used to study membrane interactions of amyloidogenic peptides (9, 14, 19).

Fig. 1a shows the kinetic profiles of hIAPP fibril formation in the presence of LUVs, measured by the commonly used thioflavin T (ThT) assay (20). These profiles are characterized by a lag phase and a sigmoidal transition, as commonly observed in kinetic traces of hIAPP fibril formation (21–23). The high ThT fluorescence in the first minutes is ascribed to initial ThT binding to the microtiter plate surface. The three kinetic profiles rep-
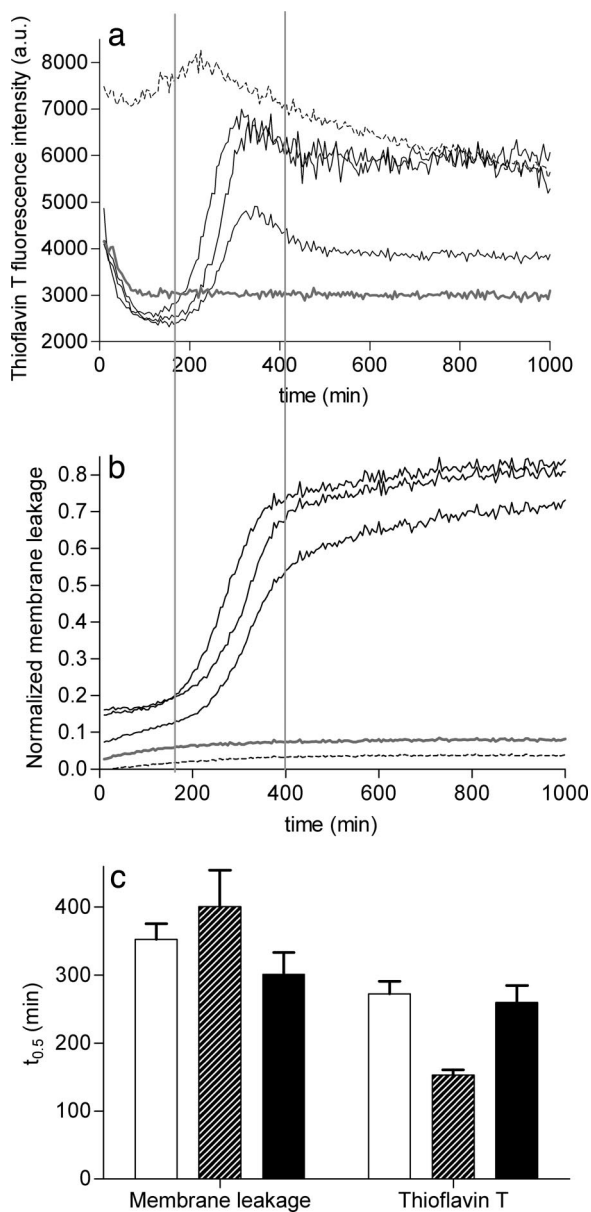
BIOPHYSICS

Fig. 1. Comparison of the kinetics of hIAPP fibril growth and hIAPP-induced membrane leakage. (*a* and *b*) ThT fluorescence (*a*) and membrane leakage (*b*) were measured independently after the addition of hIAPP at a final concentration of 5 μM to DOPC/DOPS 7:3 LUVs (43 μM lipids) at time *t* = 0. The three solid black lines represent three hIAPP samples measured at the same time, in three adjacent wells on the same microtiter plate, with the same stock solutions. Representative traces are shown for mIAPP (gray lines) and preformed hIAPP fibrils (dashed lines). The two vertical lines are shown to facilitate comparison of the kinetic traces in *a* and *b*. (*c*) The average midpoints ($t_{0.5}$) of the sigmoidal transitions for both ThT fluorescence and membrane leakage were obtained by fitting the curves to a standard sigmoidal function (see *Experimental Procedures*) and are shown for three independent experiments, each performed in triplicate, on different days, with different hIAPP stock solutions. The black bars correspond to the two experiments shown in *a* and *b*. The error bars indicate the standard deviation.

resent three simultaneous experiments performed in three adjacent wells of a microtiter plate with the same hIAPP and LUV stock solutions. These three profiles demonstrate the stochastic variability in lag times that is characteristic for nucleation-dependent aggregation processes (24, 25). Control experiments show that, under the experimental conditions used, the ThT

fluorescence of mouse IAPP (mIAPP) remains low, as expected for this nonfibrillogenic peptide, whereas the ThT fluorescence of preformed hIAPP fibrils remains high during incubation with LUVs (Fig. 1*a*). The presence of a lag phase of 1–4 h in the kinetics of hIAPP fibril formation in the presence of LUVs was also observed in a negative-stain electron microscopy experiment in which aliquots were taken, at different time points, from a sample in which hIAPP was incubated with LUVs [supporting information (SI) Fig. S1]. Next, membrane leakage experiments were performed under the same conditions as used for fibril formation. Fig. 1*b* shows that the kinetic profiles of membrane leakage are similar to those of fibril formation, also being characterized by a lag phase and a sigmoidal transition. The relatively low leakage, immediately and shortly after the addition of hexafluoroisopropyl alcohol (HFIP)-treated hIAPP to the LUVs, indicates that monomeric hIAPP does not cause membrane damage. Importantly, both mIAPP and preformed hIAPP fibrils cause only low membrane leakage (Fig. 1*b*). Fig. 1*c* illustrates that the variation in lag times between simultaneous experiments with the same hIAPP stock solution is small compared with those between independent experiments. Yet, there is a clear overlap in lag times between leakage and fibril formation, as indicated by the similar values for the midpoints ($t_{0.5}$) of the sigmoidal transitions. The results even suggest that fibril formation may slightly precede membrane damage. In any case, it can be concluded that membrane leakage is directly related to the process of fibril formation and that neither mature fibrils nor monomeric IAPP species are responsible for membrane leakage.

It has been shown that the lag time of hIAPP fibril formation in the presence of lipids is sensitive to both the hIAPP:lipid ratio and the fraction of negatively charged lipids (22, 26). Therefore, if indeed membrane leakage is linked to fibril growth, these variables should also affect the lag time of hIAPP-induced membrane damage. Decreasing the hIAPP concentration at constant lipid concentration results in a similar increase of the duration of the lag time for both fibril formation and membrane leakage (Fig. S2). The final level of hIAPP-induced membrane leakage, after a 2,000-min incubation, does not depend on the presence of 1,2-dioleoyl-*sn*-glycero-3-phospho-L-serine (DOPS), and is consistently low for both mIAPP and preformed hIAPP fibrils (Fig. S3). Yet, in the absence of DOPS, the lag time of hIAPP-induced leakage significantly increases (Fig. S3 *Inset*), matching the effect on hIAPP fibril formation (22, 26). Thus, these observations also support a direct link between hIAPP-induced membrane damage and fibril formation.

Seeding Reduces the Lag Time of hIAPP-Induced Membrane Damage.
To test whether hIAPP-induced membrane damage is caused by hIAPP fibril growth, we performed the vesicle leakage assay in the presence of small amounts of preformed hIAPP seeds. Acceleration of membrane leakage in the presence of seeds would be expected if hIAPP fibril growth causes membrane damage because seeding decreases the lag time of hIAPP fibril formation (21, 27). However, seeding should not accelerate membrane leakage if oligomers were the cause of membrane damage because seeding does not accelerate oligomer formation, due to structural differences between fibrils and oligomers (28). Fig. 2 shows that the addition of hIAPP seeds, at concentrations ranging from 1 to 10%, significantly shortens the lag time of hIAPP-induced leakage in a concentration-dependent manner. This effect on the lag time of the addition of 1–10% seeds is much more than would be anticipated from only increasing the hIAPP concentration with the equivalent of 0.05–0.5 μM, respectively (Fig. S2). These results suggest that it is elongation of the seeds, i.e., fibril growth, and not the action of an intermediate oligomeric species of hIAPP, that is responsible for promoting membrane leakage.
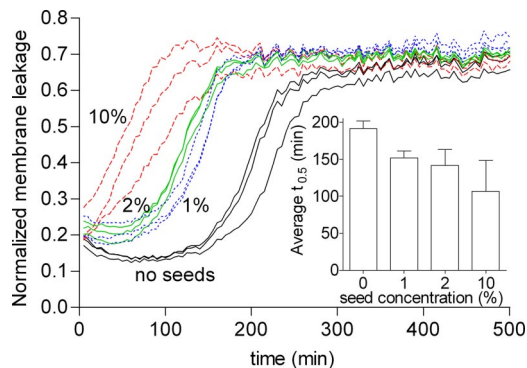
Fig. 2. Effect of seeding on hIAPP-induced membrane leakage. Kinetic curves of membrane leakage without (black lines) and with 1% (dotted blue lines), 2% (green lines), and 10% (dashed red lines) hIAPP seeds. The three lines of the same color represent three samples measured at the same time in three adjacent wells on the same microtiter plate with the same stock solutions. (*Inset*) Comparison of the average $t_{0.5}$ of three independent experiments, each performed in triplicate. The error bars indicate the standard deviation.

Insulin Protects Against hIAPP-Induced Membrane Damage. If our hypothesis is correct, i.e., if hIAPP fibril growth causes membrane damage, then one would predict that inhibition of hIAPP fibril growth would also inhibit hIAPP-induced membrane leakage. To test this, we have chosen insulin as a biologically relevant, potent inhibitor of hIAPP fibril formation (29–31). The mechanism of inhibition of hIAPP fibril formation by insulin is most likely related to strong binding of the insulin B-chain to hIAPP (32). We find that coincubation of insulin with hIAPP and calcein-loaded LUVs indeed has a significant protecting effect on hIAPP-induced membrane damage. At a hIAPP:insulin ratio of 1:1, membrane leakage after 1,000 min is reduced to 0.65 ± 0.16, whereas at a more physiological hIAPP:insulin ratio of 1:10 the membrane leakage is reduced further to only 0.28 ± 0.03.

Individual hIAPP Fibrils Are Associated with Distorted Phospholipid Vesicles. Finally, if indeed fibril growth at the membrane would be responsible for membrane leakage, one would also expect that growing hIAPP fibrils are in physical contact with LUVs to be able to cause such membrane damage. To investigate this possibility, cryo-transmission electron microscopy (cryo-TEM) was used to visualize the interaction between hIAPP and LUVs. Fig. 3*a* shows that after incubating hIAPP with LUVs, individual hIAPP fibrils are formed that line the surface of LUVs (see also Figs. S4 and S5 *c* and *d*). The size and morphology of these fibrils are similar to those of hIAPP fibrils formed in the absence of LUVs (Fig. 3*b*). In both cases, hIAPP forms straight, unbranched fibrils with a width of 10–15 nm and a length of 0.5–1 μm, characteristic of hIAPP amyloid fibrils (33, 34). An additional interesting feature in the micrographs is that most of the LUVs that are in contact with hIAPP fibrils show distorted, noncircular shapes (asterisks in Fig. 3*a* and Figs. S4 and S5 *c and d*). These distorted LUVs comprise ≈10% of the total number of LUVs present. This distortion of the vesicle shape must be related to fibril formation because in the presence of the nonamyloidogenic mIAPP, fibril-like structures are absent and all LUVs have a well defined circular shape (Fig. 3*c*). These LUVs are indistinguishable from LUVs in the absence of peptide (results not shown). Distorted LUVs are absent or only incidentally present when preformed mature hIAPP fibrils are added to LUVs (Fig. S5 *a and b*). These results suggest that fibril formation at the membrane surface may lead to vesicle distortion. It is possible that such a distortion is directly responsible for
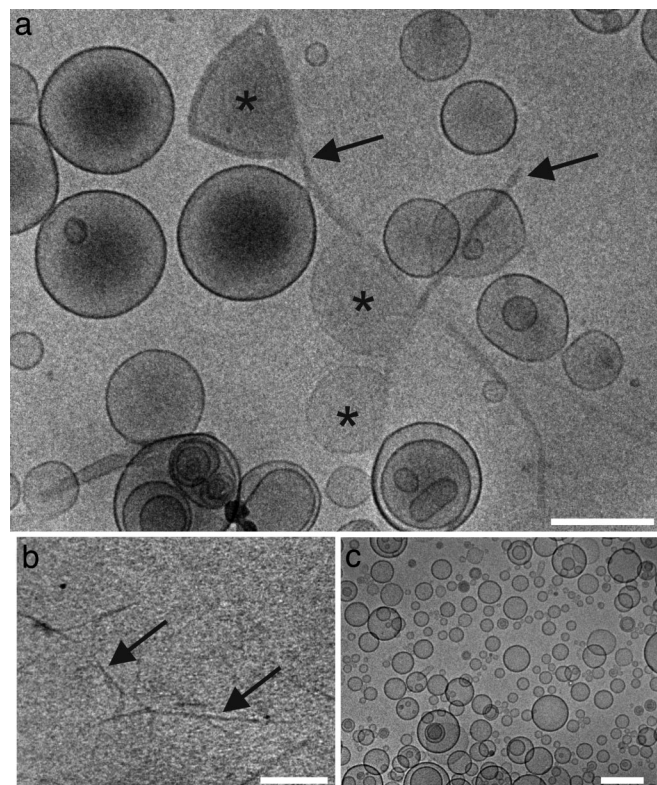

Fig. 3. Cryo-TEM of the interaction of hIAPP and mIAPP with LUVs. (*a*) hIAPP in the presence of LUVs. (*b*) hIAPP fibrils in the absence of LUVs. (*c*) mIAPP in the presence of LUVs. Distorted LUVs (asterisks) are in contact with hIAPP fibrils (black arrows). All samples contain 5% DMSO. LUVs are composed of DOPC/DOPS 7:3 with a phospholipid concentration of 7 mM. IAPP concentration is 1 mM. (Scale bars, 200 nm.)

membrane leakage, providing a potential mechanistic link between the processes of membrane damage and fibril growth.

Discussion

By studying the kinetics of hIAPP-induced membrane damage and hIAPP fibril growth with a model membrane system, we have obtained many independent indications that fibril growth and membrane damage are intimately linked. First, we observed that the kinetic profile of hIAPP-induced membrane leakage, characterized by a lag phase and a sigmoidal transition, matches that of hIAPP fibril formation. Second, the addition of hIAPP seeds, which are shown to accelerate hIAPP fibril growth, also accelerates hIAPP-induced membrane damage. Furthermore, a number of variables that are also known to affect hIAPP fibril formation, i.e., the presence of a fibril formation inhibitor, hIAPP concentration, and membrane lipid composition, were found to have the same effect on hIAPP-induced membrane damage. In addition, the cryo-TEM results show the physical connection between membrane damage and fibril growth. Our results favor a mechanism in which hIAPP-induced membrane damage is caused by growth of hIAPP fibrils at the membrane, as will be discussed below.

Fibril Growth vs. Oligomers as Cause of Membrane Damage. Our results show that neither hIAPP monomers nor hIAPP fibrils cause membrane damage. Consequently, either an intermediate hIAPP species ("oligomer") or the growth of hIAPP fibrils is responsible for membrane damage. The prevailing view in literature is that hIAPP oligomers cause membrane damage and that they represent the cytotoxic species responsible for β cell
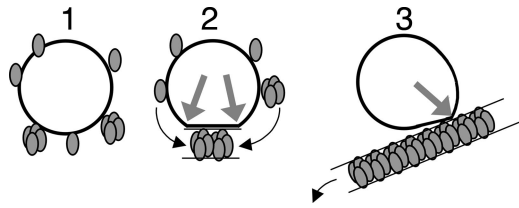
Fig. 4. Simplified schematic representation of the different stages of the proposed membrane-associated hIAPP fibril growth that results in membrane damage. Starting from a situation with an intact membrane (black circle) and monomeric hIAPP (gray ellipsoids), hIAPP monomers or oligomers adsorb on or insert into the membrane (*Left*). Next, membrane-located hIAPP participates in initiation and propagation of fibril growth at the membrane leading to a forced change in membrane curvature and concomitant temporal membrane leakage, at the locations where fibrils and membrane separate (gray arrows) (*Center*). Finally, mature hIAPP fibrils that line the surface of a distorted membrane start detaching, initiating recovery of vesicle shape (*Right*). Oligomers have been depicted arbitrarily as a cluster of four hIAPP monomers. Black arrows indicate the movement of hIAPP species.

death (2–9). However, under the conditions used in this work, our observations argue against oligomers as a direct cause for the observed membrane damage. First, a reduction of the lag time in membrane damage by seeding is not compatible with a direct membrane disrupting action of oligomers because seeding does not accelerate oligomer formation (28); seeding would require structural equivalence of the seed and the seeded product (25), hence preformed hIAPP fibrils can seed hIAPP fibril formation. Because toxic hIAPP oligomers are structurally different from hIAPP fibrils, as shown for example by microscopic methods (3, 5, 6) or by their different reactivity toward specific antibodies (35), they cannot be seeded by preformed hIAPP fibrils. Second, toxic oligomers are generally formed before the appearance of fibrils (3, 8), which is not compatible with our results that show fibril growth just before or at the same time as membrane damage, placing oligomer formation at an even earlier time point than membrane damage. Third, oligomeric hIAPP species were not found in our analysis of hIAPP–LUV interactions by cryo-TEM and negative-stain EM. Consequently, we conclude that not a specific hIAPP species, but the process of hIAPP fibril growth, is responsible for the observed membrane damage.

How Does hIAPP Fibril Growth Cause Membrane Damage? Fig. 4 presents a simplified schematic representation of the different stages of the membrane-associated process of hIAPP fibril growth that results in membrane damage, as we propose based on the results obtained here. Initially, hIAPP inserts in or adsorbs on the membrane, either as monomer or as oligomer (Fig. 4 *Left*). The interaction of monomeric hIAPP with membranes is likely because monomeric hIAPP has a strong tendency to insert in phospholipid monolayers (36, 37). In the next step, interactions of membrane-located hIAPP species with each other or with hIAPP species in solution could lead to growth of fibrils at the membrane (Fig. 4 *Center*). The membrane itself could promote hIAPP fibril growth by increasing the local concentration of (membrane-bound) hIAPP and/or by inducing a specific orientation or conformation of the peptide, which could facilitate fibril growth. The mechanism of membrane damage could entail growth of a rigid hIAPP fibril on a flexible phospholipid bilayer, which would result in a forced change in membrane curvature. This change could lead to temporal membrane disruption at the location where fibril and membrane separate (gray arrows in Fig. 4 *Center* and *Right*). Cryo-TEM pictures show this forced change by the appearance of distorted vesicles with sharpened corners at the places where membrane and fibril separate. Mature fibrils have less affinity for phospholipids than monomers (36) leading to detachment of fibrils

and recovery of vesicle shape (Fig. 4 *Right*), which would be in agreement with the observation that only 10% of the LUVs is distorted compared with 70–80% membrane leakage (Figs. 1 and 2; Figs. S2 and S3). Uptake of membrane phospholipids in amyloid that forms at the membrane, as observed from *in vitro* studies by us (12) and others (38), as well as by *in vivo* studies (39), could be an additional factor that contributes to membrane leakage.

Amyloid-Independent Membrane Damage. Next to the extensively documented role of hIAPP oligomers in membrane damage (2–9), also another model, the so-called carpet model, has been suggested (14), similar to the action of antimicrobial peptides. However, in case of amyloid diseases, the carpet model is of minor physiological relevance because it was found that both hIAPP and the nonamyloidogenic mIAPP cause similar membrane damage under specific experimental conditions (14). A carpet model could also explain the exponential leakage kinetics and absence of lag phase in both hIAPP- and mIAPP-induced leakage of LUVs composed solely of negatively charged lipids (9). This model might also explain the relatively small (0.05–0.2) initial leakage present at the first minutes after the addition of hIAPP (Figs. 1 and 2; Fig. S2) and the leakage (0.15) induced by mIAPP (Fig. 1; Fig. S3). Consequently, fibril growth at the membrane is the main mechanism of the amyloid-induced membrane damage observed here, whereas the carpet model to some extent might explain fibril growth-independent membrane damage.

Membrane Damage by Fibril Growth *in Vivo*. Membrane damage of β cells by hIAPP fibril growth at the membrane could be initiated by changes in cellular conditions as a result of a (pre)diabetic state, for instance, a change in the hIAPP:insulin ratio (30) or an increase in the amount of negatively charged membrane lipids (40). *In vivo*, hIAPP is secreted from β cell secretory vesicles together with insulin, in a ratio of ≈1:10 (30). At this ratio, we have observed that insulin is able to inhibit hIAPP-induced membrane damage. Consequently, insulin could play a role as a natural inhibitor of hIAPP-induced membrane damage. Recently, it was shown that insulin also protects cells against the cytotoxic action of Abeta, the peptide that forms amyloid fibrils in Alzheimer's disease (41). Interestingly, protection by insulin was connected to the ability of insulin to inhibit both Abeta fibril formation and Abeta–membrane interaction (41). Inhibition of hIAPP-induced membrane damage by insulin, an efficient inhibitor of hIAPP fibril formation, is another argument for the causal role of hIAPP fibril growth.

In a cellular environment, hIAPP-induced morphological changes of cellular membranes, like disruption, blebbing, or vesicle budding, have frequently been observed (7, 42–47). These interesting observations indicate that *in vivo* membrane distortions and membrane damage also could be linked to fibril growth at the membrane.

In conclusion, several independent observations indicate that hIAPP-induced membrane damage is caused by hIAPP fibril growth at the membrane. Our hypothesis may also be relevant for elucidation of the mechanism of membrane damage by other amyloidogenic peptides, such as the Alzheimer's disease-related Aβ and the Parkinson's disease-related α-synuclein.

Experimental Procedures

Materials. Synthetic hIAPP was obtained from Bachem, lot nos. 0564591 and 2500000. Synthetic mIAPP was obtained from Pepscan Systems. The calculated mass of the peptides was confirmed by mass spectrometry. 1,2-Dioleoyl-*sn*-glycero-3-phosphocholine (DOPC) and DOPS were obtained from Avanti Polar Lipids. Bovine insulin and ThT were obtained from Sigma.

Engel *et al.*

Preparation of Peptide Samples. Peptide stock solutions were prepared by dissolving a weighed amount of freeze-dried peptide powder in the respective solvent. hIAPP and mIAPP were dissolved at a concentration of 1 mM in HFIP and incubated for at least 1 h. Next, HFIP was evaporated by using a gentle stream of dry nitrogen followed by vacuum desiccation for 20 min. The resulting peptide film was then dissolved in DMSO to a final peptide concentration of 1 or 2 mM. hIAPP stock solutions in DMSO with a concentration of 0.2 and 0.02 mM were prepared by diluting the stock solutions. All peptide stock solutions were prepared in nonstick Eppendorf tubes (Alpha Laboratories). hIAPP seeds were prepared from HFIP-treated hIAPP stock solutions in DMSO, described above, by using a modified version of a known protocol (21). Seeds were produced by diluting a 1 mM hIAPP stock solution to a concentration of 50 μM in 10 mM Tris·HCl + 100 mM NaCl at pH 7.4 and incubating for 16–17 h at room temperature. This period is sufficient to produce hIAPP fibrils, as confirmed by electron microscopy and ThT fluorescence. Next, the seeds were diluted five times to a concentration of 10 μM in the same buffer and kept at room temperature for a maximum of 2 h. The Eppendorf tube with 100 μl of seed solution was sonicated for 2 min in a bath sonicator (Branson model 1200; Branson Ultrasonics). Seeds were used within 15 min of sonication and added to the LUVs 5–10 min before the addition of hIAPP. Just before adding the seeds to the LUVs, the seed solution was pipetted up and down to ensure a homogeneous sample. hIAPP fibrils were prepared by diluting a 1 mM hIAPP stock solution to a concentration of 50 μM in 10 mM Tris·HCl + 100 mM NaCl at pH 7.4 and incubating for at least 1 night at room temperature. Fibrils were diluted five times with the same buffer. Fibrils for the cryo-EM experiment at a peptide concentration of 100 μM were prepared at a concentration of 110 μM and diluted to 100 μM before the experiment. Just before use, fibril suspensions were vortexed. Fibrils and seeds were prepared in standard 1.5-ml Eppendorf tubes without stirring. Insulin was dissolved in DMSO at a peptide concentration of 1 mM.

Preparation of LUVs. The LUVs are composed of DOPC/DOPS in a 7:3 molar ratio. For further information, see *SI Materials and Methods*.

Membrane Leakage Experiments. Membrane damage was quantified *in situ* by allowing hIAPP fibril formation in the presence of calcein-filled LUVs. This is an established membrane leakage assay, routinely used to measure membrane damage induced by, for example, antibacterial peptides (48). A plate reader (Spectrafluor; Tecan) was used to perform the leakage experiments in standard 96-wells transparent microtiter plates. The leakage assay was started by adding 5 μl of a 0.2 mM hIAPP stock solution in DMSO to 195 μl of a mixture of calcein containing LUVs (43 μM lipids) and 10 mM Tris·HCl, 100 mM NaCl at pH 7.4. The DMSO concentration of all samples was matched to 2.5% (vol/vol). Directly after the addition of all components, the microtiter plate was shaken for 9 s by using the shaking function of the plate reader. The plate was not shaken during the measurement. Fluorescence was measured from the top, every 5 min, by using a 485-nm excitation filter and a 535-nm emission filter. The temperature during the measurement was 28 ± 3°C. The maximum

leakage at the end of each measurement was determined by adding 1 μl of 10% Triton X-100 to a final concentration of 0.05% (vol/vol). Deposition of fibrils on the bottom of the wells and/or a lower liquid level in the wells because of evaporation (fluorescence is measured from the top of the wells) causes the slight decrease in ThT fluorescence intensity observed during the measurement. Leakage assays at a peptide concentration of 0.1 mM and a lipid concentration of 0.9 mM were performed in a quartz microcuvette (volume of 100 μl) without stirring, by using a fluorometer at excitation and emission wavelengths of 492 and 510 nm, respectively, and excitation and emission band pass of 0.5 and 5 nm, respectively. The leakage assay was started by adding 5 μl of a 2 mM hIAPP stock solution in DMSO to 95 μl of a mixture of calcein containing LUVs (0.9 mM lipids) and 10 mM Tris·HCl, 100 mM NaCl at pH 7.4. The DMSO concentration of all samples was matched to 5% (vol/vol). The temperature during the measurement was 20 ± 1°C. The maximum leakage at the end of each measurement was determined by adding 2 μl of 10% Triton X-100 to a final concentration of 0.1% (vol/vol).

The release of fluorescent dye was calculated according to Eq. **1**,

$$L(t) = (F_t - F_0)/(F_{100} - F_0), \qquad [1]$$

where $L(t)$ is the fraction of dye released (normalized membrane leakage), F_t is the measured fluorescence intensity, and F_0 and F_{100} are the fluorescence intensities at times $t = 0$, and after addition of Triton X-100, respectively.

ThT Assay. The kinetics of hIAPP fibril formation was measured by using the fluorescence intensity increase upon binding of the fluorescent dye ThT to hIAPP fibrils, a commonly used method to detect amyloid fibrils (20). A plate reader (same as for leakage experiments) was used to perform ThT experiments in standard 96-well flat-bottom black microtiter plates in combination with a 430-nm excitation filter and a 535-nm emission filter. The conditions for the ThT experiments were the same as for the leakage experiments, except for the presence of 10 μM ThT and the absence of calcein. ThT assays at a peptide concentration of 0.1 mM and a lipid concentration of 0.9 mM were performed in a quartz microcuvette without stirring, by using a fluorometer at excitation and emission wavelengths of 450 and 482 nm, respectively, and both excitation and emission band pass at 5 nm. The conditions for these ThT experiments were the same as for the leakage experiments at 0.1 mM peptide, except for the presence of 10 μM ThT and the absence of calcein. Measurement of ThT intensity of hIAPP fibril formation in the presence of calcein filled LUVs leads to erroneous results because of the overlapping excitation and emission spectra of calcein and ThT.

Data Analysis. See *SI Materials and Methods*.

Electron Microscopy. See *SI Materials and Methods*.

1. Höppener JWM, Ahrén B, Lips CJM (2000) Islet amyloid and type 2 diabetes mellitus. *N Engl J Med* 343:411–419.
2. Mirzabekov TA, Lin MC, Kagan, BL (1996) Pore formation by the cytotoxic islet amyloid peptide amylin. *J Biol Chem* 271:1988–1992.
3. Quist A, *et al*. (2005) Amyloid ion channels: A common structural link for protein-misfolding disease. *Proc Natl Acad Sci USA* 102:10427–10432.
4. Anguiano M, Nowak RJ, Lansbury PT, Jr (2002) Protofibrillar islet amyloid polypeptide permeabilizes synthetic vesicles by a pore-like mechanism that may be relevant to type II diabetes. *Biochemistry* 41:11338–11343.
5. Porat Y, Kolusheva S, Jelinek R, Gazit E (2003) The human islet amyloid polypeptide forms transient membrane-active prefibrillar assemblies. *Biochemistry* 42:10971–10977.
6. Kayed R, *et al*. (2004) Permeabilization of lipid bilayers is a common conformation-dependent activity of soluble amyloid oligomers in protein misfolding diseases. *J Biol Chem* 279:46363–46366.
7. Janson J, *et al*. (1999) The mechanism of islet amyloid polypeptide toxicity is membrane disruption by intermediate-sized toxic amyloid particles. *Diabetes* 48:491–498.
8. Meier JJ, *et al*. (2006) Inhibition of hIAPP fibril formation does not prevent beta-cell death: Evidence for distinct actions of oligomers and fibrils of hIAPP. *Am J Physiol* 291:E1317–E1324.
9. Knight JD, Hebda JA, Miranker AD (2006) Conserved and cooperative assembly of membrane-bound α-helical states of islet amyloid polypeptide. *Biochemistry* 45:9496–9508.
10. Kourie JI, (2002) Heterogeneous amyloid-formed ion channels as a common cytotoxic mechanism: Implications for therapeutic strategies against amyloidosis. *Cell Biochem Biophys* 36:191–207.
11. Arispe N, Pollard HB, Rojas E (1993) Giant multilevel cation channels formed by Alzheimer disease amyloid β-protein [Aβ P-(1–40)] in bilayer membranes. *Proc Natl Acad Sci USA* 90:10573–10577.
12. Sparr E, *et al*. (2004) Islet amyloid polypeptide-induced membrane leakage involves uptake of lipids by forming amyloid fibers. *FEBS Lett* 577:117–120.
13. Demuro A, *et al*. (2005) Calcium dysregulation and membrane disruption as a ubiquitous neurotoxic mechanism of soluble amyloid oligomers. *J Biol Chem* 280:17294–17300.
14. Green JD, *et al*. (2004) Atomic force microscopy reveals defects within mica supported lipid bilayers induced by the amyloidogenic human amylin peptide. *J Mol Biol* 342:877–887.
15. Brender JR, *et al*. (2007) Membrane fragmentation by an amyloidogenic fragment of human islet amyloid polypeptide detected by solid-state NMR spectroscopy of membrane nanotubes. *Biochim Biophys Acta* 1768:2026–2029.
16. Okada T, Wakabayashi M, Ikeda K, Matsuzaki K (2007) Formation of toxic fibrils of Alzheimer's amyloid β-protein-(1–40) by monosialoganglioside GM1, a neuronal membrane component. *J Mol Biol* 371:481–489.
17. Novitskaya V, Bocharova OV, Bronstein I, Baskakov IV (2006) Amyloid fibrils of mammalian prion protein are highly toxic to cultured cells and primary neurons. *J Biol Chem* 281:13828–13836.
18. Gharibyan AL, *et al*. (2006) Lysozyme amyloid oligomers and fibrils induce cellular death via distinct apoptotic/necrotic pathways. *J Mol Biol* 365:1337–1349.
19. McLaurin J, Chakrabartty A (1996) Membrane disruption by Alzheimer β-amyloid peptides mediated through specific binding to either phospholipids or gangliosides: Implications for neurotoxicity. *J Biol Chem* 271:26482–26489.
20. LeVine H, III (1999) Quantification of β-sheet amyloid fibril structures with thioflavin T. *Methods Enzymol* 309:274–284.
21. Padrick SB, Miranker AD (2002) Islet amyloid: Phase partitioning and secondary nucleation are central to the mechanism of fibrillogenesis. *Biochemistry* 41:4694–4703.
22. Jayasinghe SA, Langen R (2005) Lipid membranes modulate the structure of islet amyloid polypeptide. *Biochemistry* 44:12113–12119.

BIOPHYSICS

23. Ruschak AM, Miranker AD (2007) Fiber-dependent amyloid formation as catalysis of an existing reaction pathway. *Proc Natl Acad Sci USA* 104:12341–12346.
24. Ferrone FA, Hofrichter J, Eaton WA (1985) Kinetics of sickle hemoglobin polymerization. II. A double nucleation mechanism. *J Mol Biol* 183:611–631.
25. Harper JD, Lansbury PT (1997) Models of amyloid seeding in Alzheimer's disease and scrapie: Mechanistic truths and physiological consequences of the time-dependent solubility of amyloid proteins. *Annu Rev Biochem* 66:385–407.
26. Knight JD, Miranker AD (2004) Phospholipid catalysis of diabetic amyloid assembly. *J Mol Biol* 341:1175–1187.
27. O'Nuallain B, Williams AD, Westermark P, Wetzel R (2004) Seeding specificity in amyloid growth induced by heterologous fibrils. *J Biol Chem* 279:17490–17499.
28. Kelly JW (2000) Mechanisms of amyloidogenesis. *Nat Struct Biol* 7:824–826.
29. Westermark P, *et al.* (1996) Effects of beta cell granule components on human islet amyloid polypeptide fibril formation. *FEBS Lett* 379:203–206.
30. Jaikaran ETAS, Nilsson MR, Clark A (2004) Pancreatic beta-cell granule peptides form heteromolecular complexes which inhibit islet amyloid polypeptide fibril formation. *Biochem J* 377:709–716.
31. Kudva YC, Mueske C, Butler PC, Eberhardt NL (1998) A novel assay *in vitro* of human islet amyloid polypeptide amyloidogenesis and effects of insulin secretory vesicle peptides on amyloid formation. *Biochem J* 331:809–813.
32. Gilead S, Wolfenson H, Gazit E (2006) Molecular mapping of the recognition interface between the islet amyloid polypeptide and insulin. *Angew Chem Int Ed* 45:6476–6480.
33. Sumner Makin O, Serpell LC (2004) Structural characterisation of islet amyloid polypeptide fibrils. *J Mol Biol* 335:1279–1288.
34. Goldsbury C, *et al.* (2000) Amyloid fibril formation from full-length and fragments of amylin. *J Struct Biol* 130:352–362.
35. Kayed R, *et al.* (2003) Common structure of soluble amyloid oligomers implies common mechanism of pathogenesis. *Science* 300:486–489.
36. Engel MFM, *et al.* (2006) Islet amyloid polypeptide inserts into phospholipid monolayers as monomer. *J Mol Biol* 356:783–789.
37. Lopes DHJ, *et al.* (2007) Mechanism of IAPP fibrillation at lipid interfaces studied by infrared reflection absorption spectroscopy (IRRAS). *Biophys J* 93:3132–3141.
38. Zhao H, Tuominen EKJ, Kinnunen PKJ (2004) Formation of amyloid fibers triggered by phosphatidylserine-containing membranes. *Biochemistry* 43:10302–10307.
39. Gellermann GP, *et al.* (2005) Raft lipids as common components of human extracellular amyloid fibrils. *Proc Natl Acad Sci USA* 102:6297–6302.
40. Rustenbeck I, Matthies A, Lenzen S (1994) Lipid composition of glucose-stimulated pancreatic islets and insulin-secreting tumor cells. *Lipids* 29:685–692.
41. Rensink AAM, *et al.* (2004) Insulin inhibits amyloid β-induced cell death in cultured human brain pericytes. *Neurobiol Aging* 25:93–103.
42. Westermark P (1973) Fine structure of islets of Langerhans in insular amyloidosis. *Virchows Archiv A Pathol Anat Histopathol* 359:1–18.
43. Clark A, *et al.* (1987) Islet amyloid formed from diabetes-associated peptide may be pathogenic in type 2 diabetes. *Lancet* 330:231–234.
44. Lorenzo A, Razzaboni B, Weir GC, Yankner BA (1994) Pancreatic islet cell toxicity of amylin associated with type 2 diabetes mellitus. *Nature* 368:756–760.
45. O'Brien TD, *et al.* (1995) Human islet amyloid polypeptide expression in COS-1 cells: A model of intracellular amyloidogenesis. *Am J Pathol* 147:609–616.
46. Hiddinga HJ, Eberhardt NL (1999) Intracellular amyloidogenesis by human islet amyloid polypeptide induces apoptosis in COS-1 cells. *Am J Pathol* 154:1077–1088.
47. Saafi EL, *et al.* (2001) Ultrastructural evidence that apoptosis is the mechanism by which human amylin evokes death in RINm5F pancreatic islet beta-cells. *Cell Biol Int* 25:339–350.
48. Hasper HE, *et al.* (2006) An alternative bactericidal mechanism of action for lantibiotic peptides that target lipid II. *Science* 313:1636–1637.